This article has been accepted for publication in a future issue of this journal, but has not been fully edited. Content may change prior to final publication. Citation information: DOI 10.1109/JLT.2017.2707179, Journal of Lightwave Technology

Efficient Chromatic Dispersion Compensation and Carrier Phase Tracking for Optical Fiber FBMC/OQAM Systems

Trung-Hien Nguyen, François Rottenberg, *Student Member*, *IEEE*, Simon–Pierre Gorza, Jérome Louveaux, *Member*, *IEEE* and François Horlin, *Member, IEEE*

***Abstract*—Offset-QAM-based filterbank multicarrier (FBMC/OQAM) is an attractive candidate to improve the spectral containment of optical fiber communication systems, especially when considering a sufficiently high number of subcarriers. As for other multicarrier modulations, the chromatic dispersion (CD) compensation is simplified in FBMC/OQAM systems since it is performed in the frequency domain. Unfortunately, FBMC/OQAM systems are sensitive to the laser phase noise (PN). The PN becomes difficult to mitigate when the number of subcarriers increases due to the increased symbol period. It results in inter-carrier interference (ICI) and inter-symbol interference (ISI) due to the loss of OQAM orthogonality. In this paper, we consider the use of moderate numbers of subcarriers to allow for simpler PN tracking. Consequently, more advanced CD compensation methods are required and a trade-off between CD and PN compensations needs to be studied. In this paper, the frequency sampling equalizer is used for the CD compensation, whereas an innovative adaptive maximum likelihood estimator is used for the PN compensation. A methodology is then presented to analyze this performance trade-off between CD and PN compensations, and design the desirable system parameters such as the number of subcarriers and the equalizer length. This is illustrated in the case of a terrestrial long-haul FBMC/OQAM transmission system, with 400-kHz laser linewidth and a 1000 km optical link.**

***Index Terms*—Filter-bank multicarrier, offset QAM, coherent detection, carrier phase estimation, CD compensation, long-haul communications.**

I. Introduction

In order to satisfy the ever-increasing network capacity demands, multicarrier modulations have currently been receiving increased attention in optical fiber communication systems [1-4]. Among multicarrier modulations, offset-QAM-based filterbank multicarrier (FBMC/OQAM) has become a promising candidate to improve the spectral efficiency (SE) of optical fiber wavelength-division multiplexing (WDM) communication systems [2]. FBMC/OQAM requires no cyclic prefix compared to the optical orthogonal frequency-division multiplexing (OFDM) modulation, which improves its throughput rate. Furthermore, FBMC/OQAM exhibits a much better spectral containment than OFDM thanks to the use of a time-frequency well-localized shaping filter [3]. By using a sufficiently high number of subcarriers, the guard band inserted between two optical channels can be kept as low as tens of MHz [2], again improving the SE.

As in common multicarrier systems, using a high number of subcarriers provides a simple way to compensate for channel time dispersion generated by the chromatic dispersion (CD) with the use of a one-tap equalizer on a per-subcarrier basis. However, multicarrier systems become more sensitive to the time varying effects of the channel such as laser phase noise (PN) when the number of subcarriers increases due to the increased symbol duration. The PN causes inter-carrier interference (ICI) and inter-symbol interference (ISI) due to the loss of the OQAM orthogonality. Several new carrier phase estimation (CPE) algorithms to compensate for PN have been proposed for OQAM modulations. In the tens of GHz bandwidth of optical multicarrier systems with a laser linewidth in the commercial range (tens of kHz to several MHz), most of CPE algorithms have been validated in FBMC systems using a small number of subcarriers ($2M < 8$, where M is half number of subcarriers), such as the modified blind phase search algorithm (M-BPS) [5] and its reduced complexity versions [6-7]. We have recently proposed a frequency-domain M-BPS algorithm that can work with a higher number of subcarriers [8], up to $2M = 1024$. The pilot tone method for the PN compensation has been proposed in [9]. However, it incurs a loss of SE. In our paper, we focus on non-data-aided (blind) PN compensation methods. Since the time domain PN compensation requires some iterations and extra interpolations in multicarrier modulations systems [10], the frequency domain compensation is preferred. As concluded in [8], the number of subcarriers should be moderate enough to ensure that the PN compensation is possible in the frequency domain.

On the other hand, the CD tolerance offered by one-tap equalizer is reduced if the fiber dispersion is high, the propagation distance is long and/or the number of subcarriers

This work is supported by the Belgian Fonds National de la Recherche Scientifique (FNRS) under Grant PDR T.1039.15.

T.-H. Nguyen, F. Rottenberg, S.-P. Gorza and F. Horlin are with OPERA department, Université libre de Bruxelles, 1050 Brussels, Belgium (e-mail: trung-hien.nguyen@ulb.ac.be; simon-pierre.gorza@ulb.ac.be; francois.horlin@ulb.ac.be).

F. Rottenberg and J. Louveaux are with ICTEAM institute, Université catholique de Louvain, 1348 Louvain-la-Neuve, Belgium (e-mail: francois.rottenberg@uclouvain.be; jerome.louveaux@uclouvain.be).

0733-8724 (c) 2016 IEEE. Personal use is permitted, but republication/redistribution requires IEEE permission. See http://www.ieee.org/publications_standards/publications/rights/index.html for more information.

This article has been accepted for publication in a future issue of this journal, but has not been fully edited. Content may change prior to final publication. Citation information: DOI 10.1109/JLT.2017.2707179, Journal of Lightwave Technology

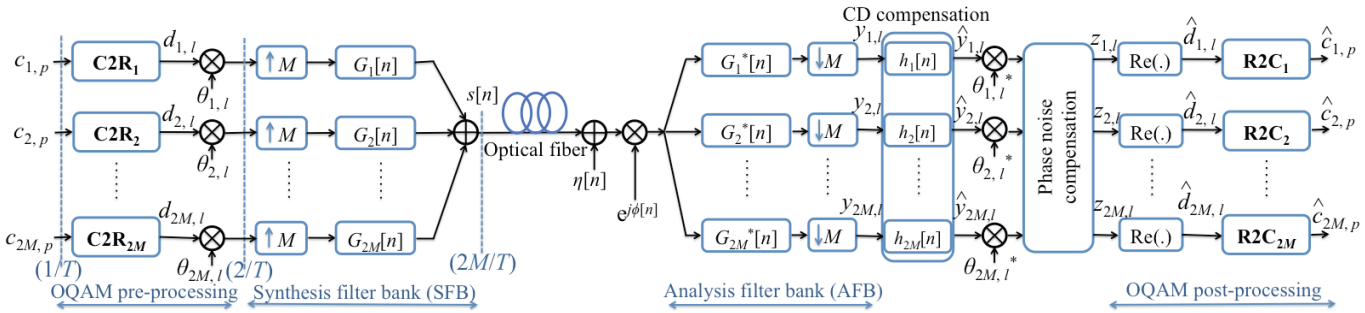


Fig. 1. FBMC/OQAM system model, considering the chromatic dispersion and laser phase noise impairments.

is low. This reduction comes from the fact that the frequency response at the subcarrier level can no longer be considered as flat when the length of the channel impulse response is long with respect to the FBMC symbol duration. Therefore, advanced methods for CD compensation are required. So far, two methods have been applied to enhance the CD tolerance. Zhao *et al.* [9] have proposed to deploy multiple analysis filter banks (AFBs) where each AFB uses a different frame synchronization. Recently, Yu *et al.* [11] have designed a three-tap equalizer to alleviate the crosstalk from the two adjacent subcarriers. One disadvantage of the former is that it requires many AFBs at the receiver to compensate for CD, while the latter uses only the information from adjacent subcarriers leading to the limited CD tolerance improvement. In wireless FBMC/OQAM communications, the frequency sampling (FS) equalizer has been shown to be an effective solution for the compensation of strong frequency selective channel [12]. To the best of our knowledge, it has not been applied to compensate for the CD in optical FBMC/OQAM systems.

In this paper, we investigate long-haul terrestrial optical fiber FBMC/OQAM systems in the presence of both CD and PN. The number of subcarriers is kept sufficiently high in order to get a high SE, i.e. at least 128 subcarriers so that discarding one subcarrier at the spectrum edge to create a guard band between two optical channels leads to less than 1% spectral loss. However, it has been shown that the number of subcarriers should not be too high to ensure that the PN can be compensated in the frequency domain, allowing for a low complexity algorithm [13]. In this work, we propose to use the FS equalizer for improving the CD tolerance. Moreover, a new simple CPE algorithm is derived from the log-likelihood function of the PN estimation. The objective of this method is to minimize the PN estimation error by using the inverted gradient descent method. This method in turn acts as an adaptive maximum likelihood estimator, referred to as AML algorithm, and it is shown to be of low complexity compared to the M-BPS. The proposed algorithms are numerically validated with 4- and 16-OQAM modulations after transmission over 1000 km of standard single-mode fiber (SSMF), with a combined laser linewidth of 400 kHz. The sampling rate is set equal to 60 GHz. Finally, we show how to optimize the FBMC/OQAM system design in terms of the performance of both CD and PN compensation and their complexity. It is shown that the number of subcarriers should be carefully chosen so that the trade-off between efficient CD and PN compensation is optimized while the complexity is kept relatively low.

The paper is organized as follows: in Section II, the FBMC/OQAM system model and its impairments are defined. In Section III, we present the FS equalizer for CD compensation and study its performance regarding the number of taps. In Section IV, we derive the PN compensation method based on the AML algorithm and investigate its performance. The hardware complexity of the proposed algorithms is discussed in Section V. In Section VI, we introduce the methodology for designing the FBMC/OQAM systems in the presence of both CD and PN effects. Finally, Section VII concludes our paper.

II. FBMC/OQAM System Model

In order to focus on the CD and PN effects, only one polarization is considered. However the extension to dual-polarization systems is straightforward. Ideal time/frequency synchronization is assumed. Fig. 1 illustrates the FBMC/OQAM system model in the presence of CD and PN. The parameters $2M$, m and T denote the number of subcarriers, subcarrier index and QAM symbol duration, respectively. At the transmitter, the QAM symbols, $c_{m,p}$, are firstly pre-processed by the OQAM block ($\mathbf{C2R}_m$), where the real and imaginary parts of QAM symbols are destaggered to form the real-valued symbols, $d_{m,l}$, at the rate $2/T$. These symbols are OQAM modulated by multiplication by a phase factor, $\theta_{m,l} = j^{m+l}$. Then the samples are M-upsampled before being filtered by the synthesis filter banks (SFB). The prototype filter, $g[n]$, has a length $L_g = 2KM$, where K is the overlapping factor. The output FBMC signal at the rate $1/T_S = 2M/T$ is obtained by the summation of all subcarriers and can be written as [14]

$$s[n] = \sum_{l=1}^{2N_S} \sum_{m=1}^{2M} d_{m,l} \cdot g_{m,l}[n], \tag{1}$$

where $g_{m,l}[n] = \theta_{m,l} \cdot g[n - lM] \cdot \exp(j\pi m/M(n - (L_g - 1)/2))$ and $2N_S$ denotes the number of real-valued multicarrier symbols (assumed to be either finite or infinite). In the simulations, we use the PHYDYAS filter as the prototype filter with overlapping factor $K = 4$ [14]. The time and frequency domain presentations of the prototype filter are shown in the inset of Fig. 2. The FBMC signal is then transmitted onto fiber links. The transfer function associated with CD, $H(f)$, can be

0733-8724 (c) 2016 IEEE. Personal use is permitted, but republication/redistribution requires IEEE permission. See http://www.ieee.org/publications_standards/publications/rights/index.html for more information.

This article has been accepted for publication in a future issue of this journal, but has not been fully edited. Content may change prior to final publication. Citation information: DOI 10.1109/JLT.2017.2707179, Journal of Lightwave Technology

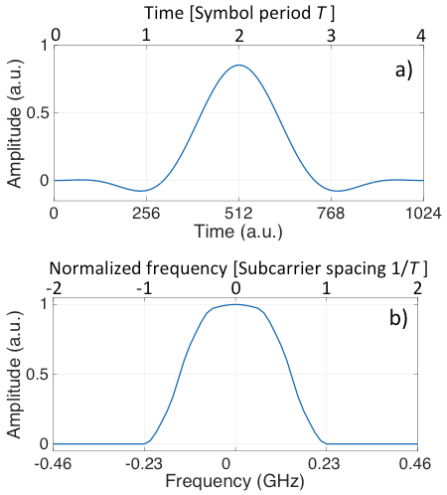


Fig. 2. Presentation of the prototype filter in a) time and b) frequency domains.

expressed as [15]

$$H(f) = e^{-j\frac{\pi D\lambda^2 L}{c}f^2}, \tag{2}$$

where L is the fiber length. The parameters λ and c denote the wavelength and speed of the light in vacuum, respectively. The parameter D represents the dispersion coefficient of the fiber. Note that, f is the relative frequency with respect to the optical carrier frequency.

The received signal, $r[n]$, is corrupted by additive circularly-symmetric white Gaussian noise (AWGN), denoted by $\eta[n]$, with zero-mean and variance N_0 and by the PN $\phi[n]$ of linewidth $\Delta\nu$. The additive noise representing the amplified spontaneous noise (ASE) of optical amplifiers and other noise sources, i.e. thermal noise, shot noise, is usually a valid assumption. The combined PN coming from transmitter and receiver lasers is modeled as a Wiener process [8]

$$\phi[n] = \phi[n-1] + \theta[n], \tag{3}$$

where $\theta[n]$ is a zero mean real Gaussian random variable with variance $\sigma_\theta^2 = \pi\cdot\Delta\nu\cdot T/M$. The received signal can be expressed as

$$r[n] = \left(\int S(f)H(f)e^{j2\pi fT_S n}\,df + \eta[n]\right)e^{j\phi[n]}, \tag{4}$$

in which $S(f)$ is the Fourier transform of $s[n]$. Assuming that the channel frequency response is approximately flat at the subcarrier level and that the phase noise is slowly varying with respect to the symbol duration, the received signal at the output of the AFB, at the subcarrier m_0 and the multicarrier symbol l_0 is given by

$$\begin{aligned} y_{m_0,l_0} &= \sum_{n=1}^{L_g} r[n]g^*_{m_0,l_0}[n] \\ &\approx e^{j\phi_{l_0}}H_{m_0}\sum_{l=1}^{2N_S}\sum_{m=1}^{2M} d_{m,l}\sum_{n=1}^{L_g} g_{m,l}[n]g^*_{m_0,l_0}[n] + w_{m_0,l_0}, \end{aligned} \tag{5}$$

where $H_m = H(f_m)$ with f_m being the m-th subcarrier frequency, w_{m_0,l_0} denotes the filtered additive noise with zero mean and variance σ_w^2 for both real and imaginary parts. Since $\mathrm{Re}\left\{\sum_{n=1}^{L_g} g_{m,l}[n]g^*_{m_0,l_0}[n]\right\} \approx \delta_{m-m_0,l-l_0}$, in which δ is the Kronecker delta function and Re is the real part operator, the received signal in (5) can be reformulated as follows

$$y_{m,l} \approx H_m\left(d_{m,l} + j\cdot u_{m,l}\right)e^{j\phi_l} + w_{m,l}, \tag{6}$$

where $u_{m,l}$ is the so-called intrinsic interference coming from the neighboring symbols on the carrier of interest. In order to obtain a simple PN estimator, we make the simplifying assumption that $u_{m,l}$ is independent of the transmitted data and has a Gaussian distribution with zero mean and variance denoted by σ_u^2. Assuming that the transmitted symbols $d_{m,l}$ are independent and of variance $E_S/2$, the variance σ_u^2 is given by

$$\sigma_u^2 = \frac{E_S}{2}\sum_{m,l}\mathrm{Im}^2\left\{\sum_{n=1}^{L_g} g_{m,l}[n]g^*_{m_0,l_0}[n]\right\}, \tag{7}$$

in which Im is the imaginary part operator. In our simulations, the signal is normalized so that the variance $E_S/2$ is set equal to 1/2. In the absence of PN, the transmitted signal can be recovered by taking $\mathrm{Re}(y_{m,l}/H_m)$. Consequently, the PN rotation should be compensated prior to the OQAM post-processing. Moreover, when the transmission distance increases and/or the number of subcarriers decreases, the assumption of a flat channel frequency response at the subcarrier level is no longer valid. This motivates the need for a more efficient CD compensation technique. Note that Fig.1 gives an intuitive understanding on the underlying principle of FBMC system and that it is efficiently implemented in this study by applying the poly phase network (PPN) and fast Fourier transform [14]. In the following sections, we discuss in details the FS equalizer for CD compensation and the proposed AML algorithm for the PN compensation.

III. Chromatic Dispersion Compensation with the Frequency Sampling Equalizer

The CD compensation method used in this paper consists in using a finite impulse response (FIR) filter applied per subcarrier (Fig. 1), whose principle is to invert the channel response at a number of target frequency points within the subchannel bandwidth. The equalizer frequency response can be calculated at the corresponding points in frequency according to the zero-forcing (ZF) criterion [12]. Hence, a FIR equalizer $h_m[n]$ can be derived by the inverse Fourier transform. The equalized signal at the receiver can be written

0733-8724 (c) 2016 IEEE. Personal use is permitted, but republication/redistribution requires IEEE permission. See http://www.ieee.org/publications_standards/publications/rights/index.html for more information.

This article has been accepted for publication in a future issue of this journal, but has not been fully edited. Content may change prior to final publication. Citation information: DOI 10.1109/JLT.2017.2707179, Journal of Lightwave Technology

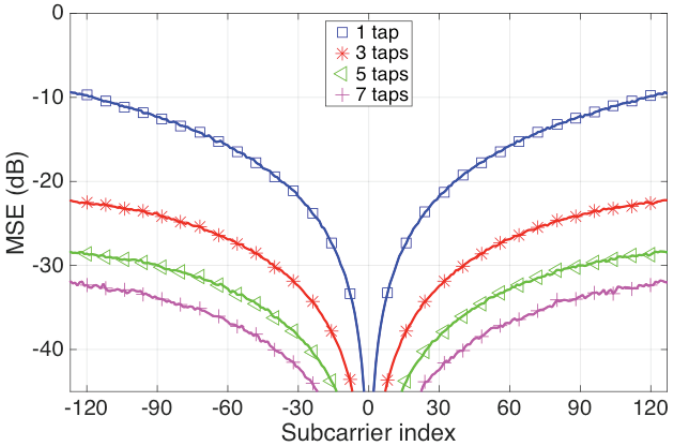


Fig. 3. MSE of the received symbols at each subcarrier index after a 1000 km optical fiber transmission, in the absence of PN and AWGN. 256 subcarriers are used.

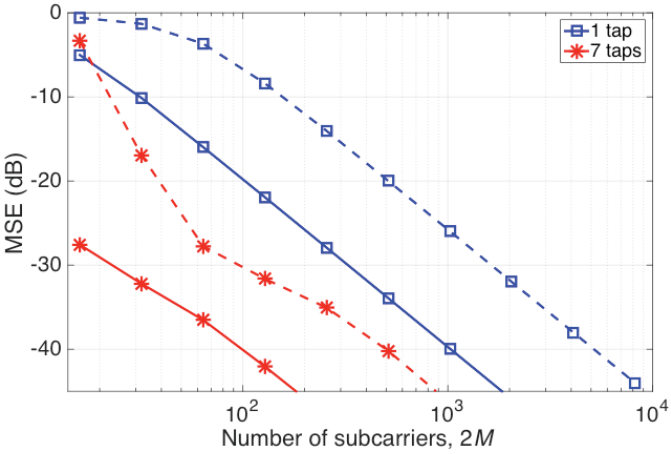


Fig. 4. MSE versus number of subcarriers, in the absence of PN and AWGN. Solid lines: 200 km, dashed lines: 1000 km.

as

$$\hat{y}_{m,l} = \sum_{l_0=0}^{N_{tap}-1} h_{m,l_0} \cdot y_{m,l_0-l+\alpha} \,, \tag{8}$$

in which N_{tap} is the number of taps of the equalizer and α is introduced to take into account the reconstruction delay. As proposed in [12], an odd number of filter taps is used in order to symmetrically control the equalizer response with respect to the subcarrier center frequency. In this case, the center frequency itself is one of the target frequency points. The equalizer can be implemented based on the knowledge of the CD. In this paper, we assume that the CD is perfectly known at the receiver. In practice, it can be acquired beforehand by using one of the existing CD estimation methods, such as [16].

To focus on the effectiveness of the FS equalizer to deal with the CD, AWGN and PN are not considered. Fig. 3 shows the mean square error (MSE) of received symbols for each subcarrier using the FS equalizer with a varying number of taps after a 1000 km optical fiber transmission. Note that, the dispersion coefficient of SSMF used in simulations is chosen equal to 17 ps/nm/km. The number of subcarriers is set to 256. The MSE exhibits the highest values on the edges of the frequency band since the phase variations of the channel are increasing with the absolute value of frequency. As it would be expected, the MSE reduces when the number of taps of the FS equalizer is increased.

Fig. 4 presents the average MSE as a function of the number of subcarriers for a 200 km and a 1000 km optical fiber transmission in the absence of AWGN and PN. In this figure, the performance of the FS equalizers with 1 tap and 7 taps are plotted. As the number of subcarriers increases, the MSE is reduced since the subcarrier width is reduced and the frequency response of the channel can be considered to be flatter at the subcarrier level. For example, in order to achieve a -28 dB MSE, if we use 1 tap equalizer and 128 subcarriers, the propagation length cannot exceed 200 km. However, using the 7 taps equalizer, a 1000 km fiber transmission achieves the same MSE by using only 64 subcarriers. The complexity of increasing the equalizer number of taps will be discussed in section V.

IV. Phase Noise Compensation Based on Inverted Gradient Descent Algorithm

Assuming that CD is completely compensated by the FS equalizer as discussed in Section III and that PN is slowly varying with respect to the symbol duration, the received signal can be re-written as

$$z_{m,l} \approx \left(d_{m,l} + j \cdot u_{m,l}\right) e^{j\phi_l} + w_{m,l} \,. \tag{9}$$

We denote by X^R (resp. X^I) the real (resp. imaginary) part of the variable X, and $(\cdot)^T$ is the transpose operator. Considering all subcarriers ($m = 1,\ldots, 2M$) at instant l, (9) can be reformulated as

$$\underline{z}_l = \underline{d}_l \otimes \underline{\phi}_l + \underline{v}_l \tag{10}$$

where the operator $\otimes$ is the Kronecker product, the received vector, the symbol vector and the PN vector are defined as

$$\begin{aligned} \underline{z}_l &= \left(z_{1,l}^R \;\; z_{1,l}^I \;\; z_{2,l}^R \;\; z_{2,l}^I \ldots z_{2M,l}^R \;\; z_{2M,l}^I\right)^T \\ \underline{d}_l &= \left(d_{1,l} \;\; d_{2,l} \ldots d_{2M,l}\right)^T \\ \underline{\phi}_l &= \left(\cos\phi_l \;\; \sin\phi_l\right)^T . \end{aligned} \tag{11}$$

The additive noise vector and its elements are defined as

$$\begin{aligned} \underline{v}_l &= \left(v_{1,l}^R \;\; v_{1,l}^I \;\; v_{2,l}^R \;\; v_{2,l}^I \ldots v_{2M,l}^R \;\; v_{2M,l}^I\right)^T \\ v_{m,l}^R &= -u_{m,l} \sin\phi_l + w_{m,l}^R \\ v_{m,l}^I &= u_{m,l} \cos\phi_l + w_{m,l}^I . \end{aligned} \tag{12}$$

It should be reminded that $u_{m,l}$ is assumed to be independent of the transmitted data and being Gaussian distributed with zero mean and variance σ_u^2. The log-likelihood function

0733-8724 (c) 2016 IEEE. Personal use is permitted, but republication/redistribution requires IEEE permission. See http://www.ieee.org/publications_standards/publications/rights/index.html for more information.

This article has been accepted for publication in a future issue of this journal, but has not been fully edited. Content may change prior to final publication. Citation information: DOI 10.1109/JLT.2017.2707179, Journal of Lightwave Technology

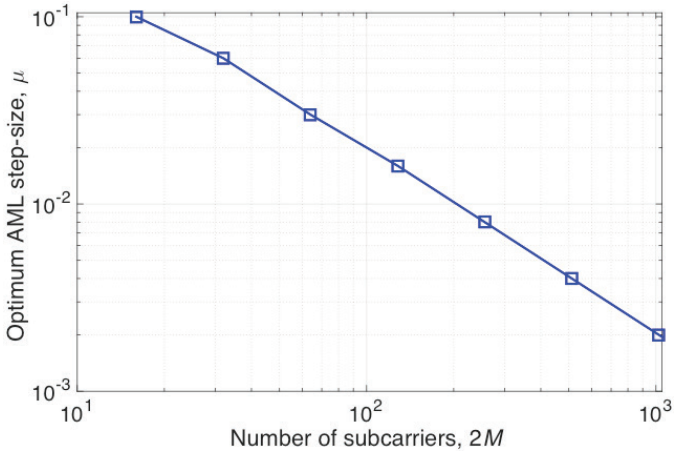


Fig. 5. Optimum AML step-size versus number of subcarriers.

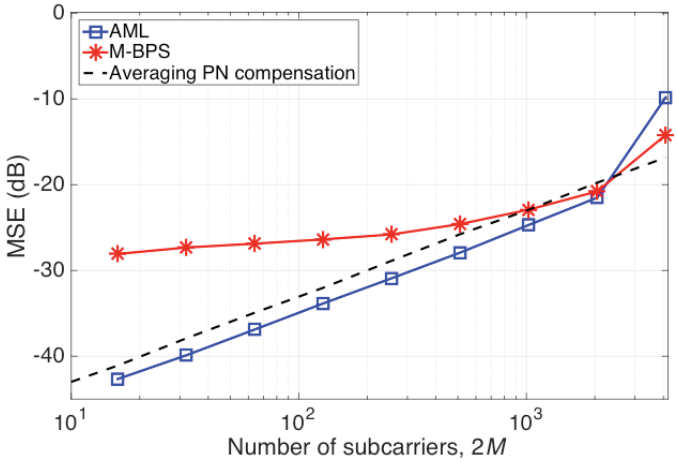


Fig. 6. MSE versus number of subcarriers using different PN compensation. Averaging PN compensation is carried out with the assumption of knowing PN.

(LLF) of $\underline{z}_l$, knowing the transmitted OQAM signals $\underline{d}_l$ and phase noise ϕ_l, has been computed in [8]

$$F(\phi_l)=\log f\left(\underline{z}_l\middle|\underline{d}_l,\phi_l\right)=C+\frac{1}{2}\sum_{m=1}^{2M}\left(\frac{|d_{m,l}|^2}{\sigma_u^2}-\frac{|z_{m,l}|^2}{\sigma_u^2+\sigma_w^2}\right)$$
$$-\frac{1}{2}\sum_{m=1}^{2M}\left(\frac{\sigma_u}{\sigma_w\sqrt{\sigma_u^2+\sigma_w^2}}\mathrm{Re}\left(z_{m,l}\cdot e^{-j\cdot\phi_l}\right)-\frac{d_{m,l}\sqrt{\sigma_u^2+\sigma_w^2}}{\sigma_u\sigma_w}\right)^2 \quad (13)$$

in which $C=-\log\left(2\pi\sigma_w\sqrt{2M\left(\sigma_u^2+\sigma_w^2\right)}\right)$. Considering a low noise case ($\sigma_w^2\ll\sigma_u^2$), the LLF becomes

$$F(\phi_l)\approx-\log\left(2\pi\sigma_w\sigma_u\sqrt{2M}\right)+\frac{1}{2\sigma_u^2}\sum_{m=1}^{2M}\left(|d_{m,l}|^2-|z_{m,l}|^2\right)$$
$$-\frac{1}{2\sigma_w^2}\sum_{m=1}^{2M}\left(\mathrm{Re}\left(z_{m,l}\cdot e^{-j\cdot\phi_l}\right)-d_{m,l}\right)^2. \quad (14)$$

The parameter ϕ_l should be selected to maximize the LLF. Equivalently, the derivative of the LLF should be equal to zero. Therefore an assessment of the LLF derivative at the current PN estimate is a measure of the PN estimate error. The derivative of the LLF, evaluated at the current estimate of the phase, is given as

$$\varepsilon_l=\sigma_w^2\left.\frac{\partial F(\phi_l)}{\partial\phi_l}\right|_{\phi_l=\hat{\phi}_l}=\sum_{m=1}^{2M}\left(-\sin\hat{\phi}_l\cdot\mathrm{Re}\left(z_{m,l}\right)+\cos\hat{\phi}_l\cdot\mathrm{Im}\left(z_{m,l}\right)\right)\times$$
$$\left(d_{m,l}-\cos\hat{\phi}_l\cdot\mathrm{Re}\left(z_{m,l}\right)-\sin\hat{\phi}_l\cdot\mathrm{Im}\left(z_{m,l}\right)\right). \quad (15)$$

We propose to use a gradient ascent approach to update the current phase estimate based on the measure of the phase error

$$\hat{\phi}_{l+1}=\hat{\phi}_l+\mu\cdot\varepsilon_l, \quad (16)$$

where μ is the step-size parameter controlling the rate of convergence, ε_l is a measure of the compensation error, obtained from (15). Since $d_{m,l}$ is not known in advance, it is estimated by direct decision of a pre-rotated version of $z_{m,l}$ with the previous PN estimate value. Note that, the use of all subcarriers for the PN estimation makes the algorithm more robust against the additive noise. Finally, the PN estimate is used to compensate for the PN effect at the next FBMC symbol.

The step-size in the adaptive maximum likelihood (AML) algorithm is a crucial parameter. It should be optimized in order to achieve the best performance of PN compensation. To study the impact of step-size on the PN compensation, the CD and AWGN are first neglected. Fig. 5 presents the optimum AML step-size as a function of the number of subcarriers. The optimum value is selected corresponding to the minimum MSE when varying the step-size. Inspection of (15) reveals that the estimation error is accumulated when increasing the number of subcarriers. This intuitively explains the reduction of the optimum step-size as the number of subcarriers increases.

Fig. 6 shows the MSE as a function of the number of subcarriers using different PN compensation methods. The "average PN compensation" is also plotted as a reference for the comparison. It is obtained, assuming that the PN is perfectly known, by computing the average of the PN on the

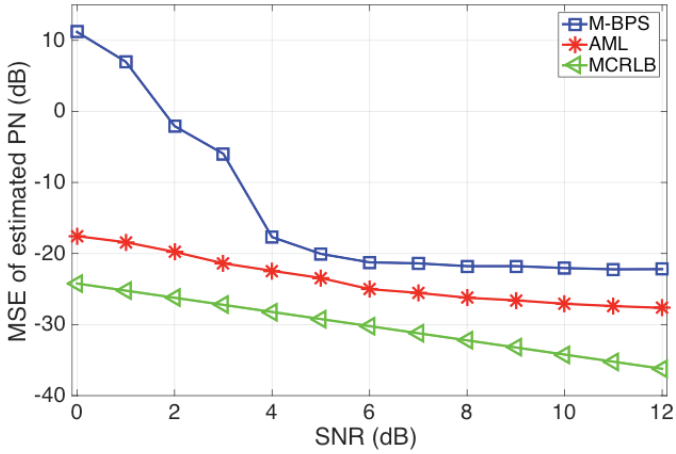


Fig. 7. MSE of the estimated PN versus SNR. Laser linewidth is set to 400 kHz and $2M$ = 256.

0733-8724 (c) 2016 IEEE. Personal use is permitted, but republication/redistribution requires IEEE permission. See http://www.ieee.org/publications_standards/publications/rights/index.html for more information.

This article has been accepted for publication in a future issue of this journal, but has not been fully edited. Content may change prior to final publication. Citation information: DOI 10.1109/JLT.2017.2707179, Journal of Lightwave Technology

TABLE I
COMPARISON OF COMPLEXITY PER REAL MULTICARRIER SYMBOL PER SUBCARRIER

Compensation method		Real multiplications	Real additions
CD compensation based on L taps FS equalizer		$4L$	$3L-1$
PN compensation	M-BPS	$2B$	B
	AML	5	3

duration of each FBMC symbol and compensating with this average value. It can be observed that a larger MSE is obtained when increasing the number of subcarriers. It is due to the fact that the symbol duration is longer when using a higher number of subcarriers, and thus the PN is no longer constant within the symbol duration making the compensation less effective. At the same time, as shown in [8], the M-BPS performance is worse for a low number of subcarriers, since there are not enough samples to average out the additive noise. Somewhat surprisingly, the AML shows better MSE than the compensation based on the true PN average, implying that the optimum value for the PN compensation of one FBMC symbol is not obtained by averaging the PN.

Fig. 7 presents the MSEs of the estimated PN using different PN compensation methods versus the signal-to-noise ratio (SNR) with the considered 400 kHz laser linewidth and $2M = 256$. The AML shows a better MSE for a large range of SNR compared to the M-BPS, which is consistent to the results in Fig. 6. Also, the modified Cramer-Rao lower bound (MCRLB) [17] is plotted as a benchmark.

It should be noted that the progressive PN update based on the previous PN estimation in the AML algorithm gets rid of using multiple phase tests as in the M-BPS algorithm. Hence, the complexity of proposed AML is obviously lower than that of M-BPS and it does not suffer from the phase quantization of M-BPS due to the limited number of phase tests. However, the performance of AML becomes worse than that of BPS for high laser linewidth or large number of subcarriers, since the assumption of the slowly varying PN is no longer valid. Details on the complexity of the PN compensation algorithm are given in Section V.

V. HARDWARE COMPLEXITY

We evaluate the complexity of different compensation algorithms in terms of multiplications and additions. Assuming that multiplying two complex numbers requires 4 real multiplications and 2 real additions, the complexity depicted in Tab. I corresponds to the number of required operations for the transmission of one real multicarrier symbol at one subcarrier. It is observed that for CD compensation, the number of multiplications and additions required by the L taps FS equalizer is proportional to L. Regarding the PN compensation, the AML reduces significantly the complexity compared to the M-BPS, as the number of phase tests B of M-BPS is generally at least equal to 16 [8].

The previous studies focus on the separated impacts of CD and PN on the FBMC/OQAM systems. In practice, the two effects are present at the same time. One can note that there exists a contradiction between the use of a high number of subcarriers for the effective mitigation of CD (Fig. 4) and the use of a relatively low number of subcarriers for the better PN compensation (Fig. 6). Moreover, the achievable performance should be traded with the complexity required by the compensation algorithms. We discuss in details in the next section the methodology for designing a long-haul FBMC/OQAM transmission system making the optimized trade-off between CD and PN compensation.

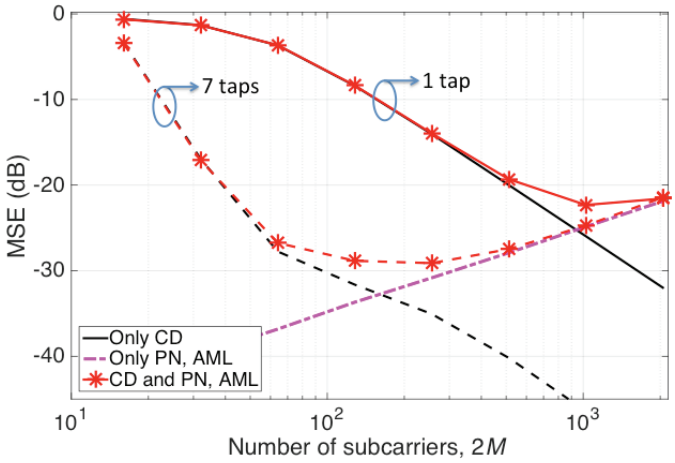


Fig. 8. Trade-off between the CD and PN compensation, 1000 km fiber and 400 kHz linewidth. Black solid lines: 1 tap equalizer; Black dashed lines: 7 taps equalizer.

VI. SYSTEM DESIGN AND DISCUSSION

The performance of a 60 GBaud FBMC system based on 4– and 16–OQAM modulations is assessed in this section in the presence of both CD and PN for a 1000 km transmission distance and a laser linewidth of 400 kHz. The number of subcarriers is considered here as a key design parameter as it directly fixes the SE in unsynchronized WDM systems using a small guard band [2]. This number is varied in order to find the best trade-off between the CD and PN compensation. Even though the transmission distance and laser linewidth are fixed in the simulations, the system design methodology still applies for different values of CD and PN. Note that we neglect the effects of the digital-to-analog converter (DAC)/ analog-to-digital converter (ADC) and analog low-pass filters in our simulations. We assume that the carrier frequency offset (CFO) is pre-compensated before the data detection can take place. Typically, the differential phase increment method proposed in [18] can perform the CFO acquisition based on the observation of dedicated training sequence.

Fig. 8 shows the trade-off between the CD and PN compensation in terms of MSE when varying the number of subcarriers. Note that no AWGN is added in the simulations in order to focus on the CD and PN impacts. The performance achieved when only one of the two effects is activated is assessed as a benchmark. Regarding the CD compensation, the performance of 1-tap equalizer (black solid lines) is compared to that of the 7-tap FS equalizer (black dashed lines).

0733-8724 (c) 2016 IEEE. Personal use is permitted, but republication/redistribution requires IEEE permission. See http://www.ieee.org/publications_standards/publications/rights/index.html for more information.

This article has been accepted for publication in a future issue of this journal, but has not been fully edited. Content may change prior to final publication. Citation information: DOI 10.1109/JLT.2017.2707179, Journal of Lightwave Technology

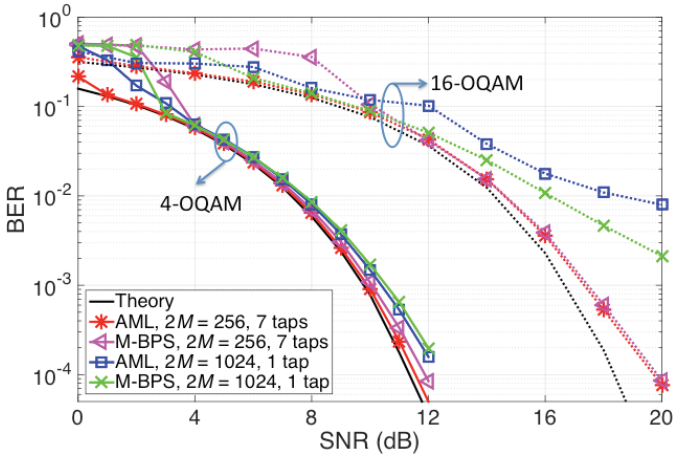


Fig. 9. BER versus SNR after 1000 km transmission with the combined laser linewidth of 400 kHz. Theory curves are achieved with only AWGN. Solid lines: 4-OQAM modulations; dotted lines: 16-OQAM modulations.

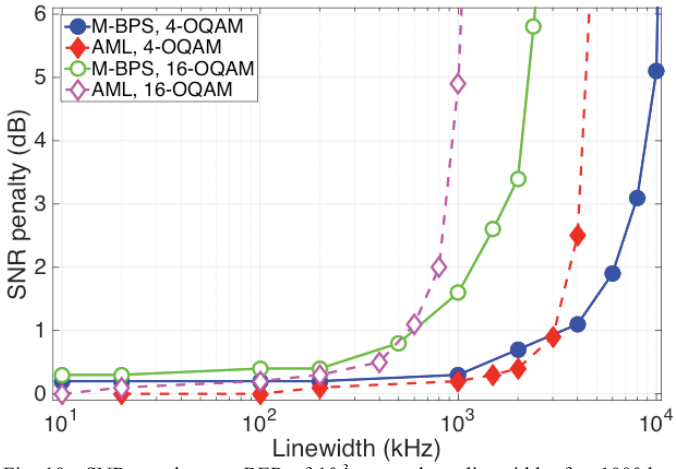


Fig. 10. SNR penalty at a BER of 10^{-3} versus laser linewidth after 1000 km transmission. 7-tap FS equalizer is used. Number of subcarriers: $2M = 256$.

Regarding the PN compensation, only the performance of the AML algorithm is illustrated as it has been shown to outperform the M-BPS algorithm for the considered laser linewidth (Fig. 6). More interestingly, the AML algorithm is of lower complexity than the M-BPS. The joint CD and PN compensation is then studied. At the receiver, the CD compensation using different numbers of equalizer taps and the PN compensation using the AML algorithm are investigated. For a low number of subcarriers, it can be seen that the 1 tap equalizer fails to recover the symbols and leads to a high MSE. For a high number of subcarriers, the performance of CD compensation is better, resulting in the reduction of MSE. As $2M$ is further increased, the PN compensation becomes less efficient resulting in an increase of the MSE. It is observed that there is an optimum compromise between CD and PN compensation regarding the number of subcarriers. Note that the exact value of the optimum number $2M$ varies depending on either the number of FS equalizer taps or the optical link parameters, i.e. optical fiber length, laser linewidth. More specifically, with the considered link configuration, the optimum number of subcarriers is 1024 when using a 1 tap equalizer and 256 when using a 7 taps equalizer.

In the next analysis, we investigate the performance of the optical link using the optimum number of subcarriers with 4- and 16-OQAM modulations. Fig. 9 shows the BER of 4- and 16-OQAM signals as a function of the SNR using AML and M-BPS algorithms. Note that, we define the SNR as the ratio between the optical signal power at the receiver input and the optical noise power over the 60 GHz system bandwidth. When $2M = 256$ and 7 taps FS equalizer are considered, no noticeable SNR penalty is observed for 4–OQAM signals while a 0.9 dB SNR penalty at the 10^{-3} BER is reported for 16–OQAM signals. If we now consider the 1–tap FS equalizer, the optimum $2M$ value is 1024 (see in Fig. 8) and we can see in Fig. 8 that the BER is worse for both 4– and 16–OQAM modulations. More particularly, the 4–OQAM modulation exhibits a 0.6 dB SNR penalty at the BER of 10^{-3}, whereas the 16–OQAM modulation cannot reach the 10^{-3} BER level regardless of the PN compensation algorithms. Note that, in the best design parameters set (corresponding to the lowest MSE) where the $2M = 256$ and 7 taps FS equalizer are used, the AML algorithm slightly outperforms the M-BPS algorithm with about 0.1 dB less SNR penalty at a BER of 10^{-3}, while the complexity of AML is lower than that of M-BPS.

In order to confirm the effectiveness of the proposed PN compensation in the laser linewidth range [10 kHz, 500 kHz] of commercial sources, we evaluate the SNR penalty to achieve a bit error rate (BER) of 10^{-3} (corresponding to the hard forward error correction (FEC) limit) as a function of laser linewidth (Fig. 10). The SNRs when considering only AWGN and no transmission to achieve a BER of 10^{-3} for 4– and 16–OQAM signals are 9.8 dB and 16.7 dB, respectively, and these values are used as the benchmarks for the SNR penalty calculation. To this evaluation, the 7 taps FS equalizer is used to compensate for the CD after 1000 km transmission and $2M = 256$. The performance of AML algorithm is compared to that of M-BPS algorithm for 4- and 16-OQAM modulations. It can be seen that the AML can provide a smaller SNR penalty than the M-BPS for systems working with laser linewidths smaller than 2 MHz and 400 kHz for corresponding 4- and 16-OQAM modulations. Considering a 1-dB SNR penalty, the tolerated linewidths of AML and M-BPS are about 3 MHz and 600 kHz for 4- and 16-OQAM

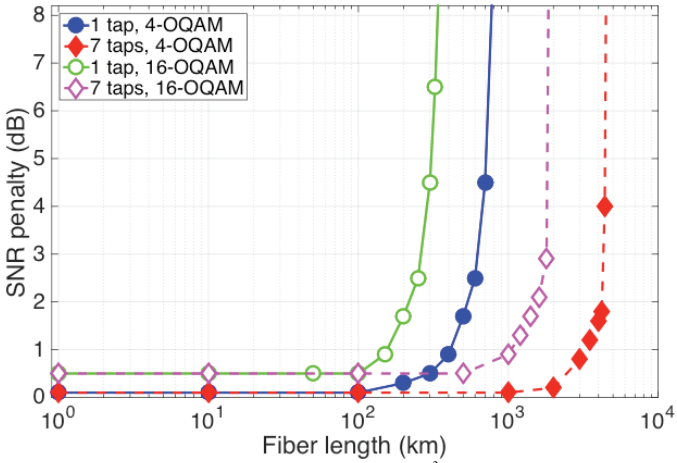


Fig. 11. SNR penalty versus fiber length at the 10^{-3} BER for 4- and 16-OQAM signals with laser linewidth $\Delta\nu = 400$ kHz and $2M = 256$.

0733-8724 (c) 2016 IEEE. Personal use is permitted, but republication/redistribution requires IEEE permission. See http://www.ieee.org/publications_standards/publications/rights/index.html for more information.

This article has been accepted for publication in a future issue of this journal, but has not been fully edited. Content may change prior to final publication. Citation information: DOI 10.1109/JLT.2017.2707179, Journal of Lightwave Technology

modulations, respectively.

A similar investigation is carried out by varying the fiber length. More specifically, we investigate the SNR penalty at a 10^{-3} BER as a function of the fiber length for 4- and 16-QAM modulations using different number of taps of the FS equalizer (Fig. 11 with $2M = 256$ and 400 kHz laser linewidth). Only AML algorithm is applied to compensate for the PN. For a 1 dB SNR penalty, the maximum reachable distances using the 1 tap equalizer are 400 km and 150 km for the 4– and 16–OQAM modulations, respectively. When the 7 taps equalizer is applied, the maximum transmission distances increase to 3200 km and 1000 km for the 4– and 16–OQAM modulations, respectively. Such results confirm the effectiveness of the proposed algorithms for CD and PN compensation. The results shown in Figs. 10 and 11 imply that, for a fixed complexity, there is a limitation in terms of linewidth and fiber length that can be handled by the system, whatever the choice of the number of subcarriers is. The only way to improve the system performance is to go towards higher complexity receivers. It is also worthwhile to note that this is also typically the point where the performance of AML starts to degrade. However, for all practical scenarios where the impact of CD and PN is mixed, AML will be better than M-BPS.

Even though the parameters of the considered systems are suitable to the terrestrial communication links, the system design rule can easily be extended to other communication links such as submarine links. For example, considering a 10 000 km transmission, the sensitivity to PN is increased in comparison to the terrestrial communication links due to the larger CD. The only way to keep an acceptable performance is to increase the number of subcarriers and possibly the number of taps of FS equalizers and to use lasers with reduced linewidth, i.e. by using 2048 subcarriers, 29 taps FS equalizer and 100 kHz laser linewidth, our numerical results show that a 60 GBaud FBMC system can reach 12000 km and 4000 km optical fiber transmission for respective 4- and 16-OQAM modulations with SNR penalties less than 1 dB at the 1.9×10^{-2} BER (corresponding to the soft FEC limit). This methodology provides an efficient way to optimize the optical FBMC/OQAM systems in terms of performance and complexity.

VII. Conclusion

We have investigated the joint CD and PN impact in optical FBMC/OQAM systems. To deal with such impairments, the simple and efficient frequency domain compensation method has been analyzed. The first one is the FS equalizer for the CD compensation and the second one is the AML algorithm for the PN compensation. The derived methods have been numerically validated with 4– and 16–OQAM modulations, confirming their effectiveness. We further discuss a methodology for the design of long haul FBMC/OQAM transmission systems in order to find the best trade-off between the performance of CD and PN compensation, and the complexity. It has been shown that the number of subcarriers is a critical parameter in the optimization of the system design. This investigation can be extended to different values of the fiber length and laser linewidth, providing an efficient way for system design.

References

[1] J. Fickers, A. Ghazisaeidi, M. Salsi, G. Charlet, P. Emplit, and F. Horlin, "Multicarrier offset-QAM for long-haul coherent optical communications," *J. Lightw. Technol.*, vol. 32, no. 24, pp. 4069-4076, Dec. 2014.

[2] Z. Li, *et al.*, "Experimental demonstration of 110-Gb/s unsynchronized band-multiplexed superchannel coherent optical OFDM/OQAM system," *Opt. Express*, vol. 21, no. 19, pp. 21924-21931, Sep. 2013.

[3] M. Bellanger, *et al.*, "FBMC physical layer: a primer," PHYDYAS project, 2010. Available: http://www.ict-phydyas.org.

[4] F. Horlin, J. Fickers, P. Emplit, A. Bourdoux, and J. Louveaux, "Dual-polarization OFDM-OQAM for communications over optical fibers with coherent detection," *Opt. Express*, vol. 21, no. 5 pp. 6409-6421, Mar. 2013.

[5] H. Tang, M. Xiang, S. Fu, M. Tang, P. Shum, and D. Liu, "Feed-forward carrier phase recovery for offset-QAM Nyquist WDM transmission," *Opt. Express*, vol. 23, no. 5, pp. 6215-6227, Mar. 2015.

[6] T.-H. Nguyen, S.-P. Gorza, J. Louveaux, and F. Horlin, "Low-complexity blind phase search for filter bank multicarrier offset-QAM optical fiber systems," in *Proc. SPPcom 2016*, Vancouver, Canada, Jul. 2016, p. SpW2G.2.

[7] J. Lu, S. Fu, H. Tang, M. Xiang, M. Tang, D. Liu, "Vertical blind phase search for low-complexity carrier phase recovery of offset-QAM Nyquist WDM transmission," Opt. Commun., vol. 382, pp. 212-218, Jan. 2017.

[8] T.-H. Nguyen, J. Louveaux, S.-P. Gorza, and F. Horlin, "Simple feedforward carrier phase estimation for optical FBMC/OQAM systems," *IEEE Photon. Technol. Lett.*, vol. 28, no. 24, pp. 2823-2826, Nov. 2016.

[9] J. Zhao and P. D. Townsend, "Dispersion tolerance enhancement using an improved offset-QAM OFDM scheme," *Opt. Express*, vol. 23, no. 13, pp. 17638-17652, Jun. 2015.

[10] X. Hong, X. Hong, and S. He, "Linearly interpolated sub-symbol optical phase noise suppression in CO-OFDM system," *Opt. Express*, vol. 23, no. 4, pp. 4691-4702, Feb. 2015.

[11] Y. Yu, P. D. Townsend, and J. Zhao, "Equalization of dispersion-induced crosstalk in optical offset-QAM OFDM systems," *IEEE Photon. Technol. Lett.*, vol. 28, no. 7, pp. 782-785, Apr. 2016.

[12] T. Ihalainen, T. H. Stitz, M. Rinne, and M. Renfors, "Channel equalization in filter bank based multicarrier modulation for wireless communications," *EURASIP J. Adv. Signal Process*, vol. 2007, Article ID 049389, Nov. 2006.

[13] B. Spinnler, "Equalizer design and complexity for digital coherent receivers," *IEEE J. Sel. Topics Quantum Electron.*, vol. 16, no. 5, pp. 1180-1192, Sep./Oct. 2010.

[14] P. Siohan, C. Siclet, and N. Lacaille, "Analysis and design of OFDM/OQAM systems based on filterbank theory," *IEEE Trans. Signal Processing*, vol. 50, no. 5, pp. 1170-1183, May 2002.

[15] S. J. Savory, "Digital coherent optical receivers: algorithms and subsystems," *IEEE J. Sel. Top. Quantum Electron.*, vol. 16, no. 5, pp. 1164-1179, Sep./Oct. 2010.

[16] H. Wymeersch, and P. Johannisson, "Maximum-likelihood-based blind dispersion estimation for coherent optical communication," *J. Lightw. Technol.*, vol. 30, no. 18, pp. 2976-2982, Sep. 2012.

[17] A. N. D'Andrea, U. Mengali, and R. Reggiannini, "The modified Cramer-Rao bound and its application to synchronization problems," *IEEE Trans. Commun.*, vol. 42, no. 2/3/4, Apr. 1994.

[18] Z. Zheng, *et al.*, "Orthogonal-band-multiplexed offset-QAM optical superchannel generation and coherent detection," *Sci. Rep.*, vol. 5, no. 17891, Dec. 2015.

0733-8724 (c) 2016 IEEE. Personal use is permitted, but republication/redistribution requires IEEE permission. See http://www.ieee.org/publications_standards/publications/rights/index.html for more information.